Dynamic polarizabilities and excitation spectra from a molecular implementation of time-dependent density-functional response theory: N_2 as a case study

Christine Jamorski, Mark E. Casida, and Dennis R. Salahub
Département de chimie, Université de Montréal, C.P. 6128, Succursale centre-ville, Montréal, Québec H3C 3J7, Canada

(Received 22 September 1995; accepted 13 November 1995)

We report the implementation of time-dependent density-functional response theory (TD-DFRT) for molecules using the time-dependent local density approximation (TDLDA). This adds exchange and correlation response terms to our previous work which used the density-functional theory (DFT) random phase approximation (RPA) [M. E. Casida, C. Jamorski, F. Bohr, J. Guan, and D. R. Salahub, in *Theoretical and Computational Modeling of NLO and Electronic Materials*, edited by S. P. Karna and A. T. Yeates (ACS, Washington, D.C., in press)], and provides the first practical, molecular DFT code capable of treating frequency-dependent response properties and electronic excitation spectra based on a formally rigorous approach. The essentials of the method are described, and results for the dynamic mean dipole polarizability and the first eight excitation energies of N_2 are found to be in good agreement with experiment and with results from other *ab initio* methods. © *1996 American Institute of Physics.* [S0021-9606(96)00408-8]

I. INTRODUCTION

Time-dependent response theory is well-known as a powerful tool for *ab initio* quantum chemical studies of molecular optics and spectroscopy. Important applications include the computation of dynamic polarizabilities and hyperpolarizabilities and electronic excitation spectra. Formulations of time-dependent response theory have been developed for a variety of *ab initio* methods, including Hartree–Fock (HF), multiconfigurational self-consistent field (MCSCF), antisymmetrized geminal power (AGP), and coupled-cluster (CC), using some variant on the Green function, polarization propagator, or equation-of-motion formalisms (see Ref. 1 for a review). More recently, a response theory formulation of second-order Møller–Plesset many-body perturbation theory (MP2) has been developed using a coupled perturbed formulation based on the Frenkel variational principle.[2,3] In view of the computational advantages of density functional theory (DFT) compared to other *ab initio* methods, combined with the good quality of DFT results for a wide variety of molecular properties, the development of a time-dependent response theory method for molecular DFT would be of clear interest. A molecular formulation of time-dependent density-functional response theory (TD-DFRT) has recently been given by one of us.[4] In a previous paper[5] we reported the first practical molecular implementation of TD-DFRT, using the DFT random phase approximation (RPA), which accounts only for the response of the coulomb terms. In the present paper, we report the molecular implementation of TD-DFRT, at the level of the time-dependent local density approximation (TDLDA), in the form of a post-deMon-KS (for ''densité de Montréal–Kohn–Sham'')[6–8] program deMon-DynaRho (for ''Dynamical Response of Rho''). As a case study, we present results for the dynamic polarizability and excitation spectrum of N_2, an important benchmark molecule for the treatment of excitations.

In a time-dependent response theory formalism, excitation spectra and polarizabilities are intimately related since the poles of the dynamic polarizability are the excitations. However, within the framework of time-independent DFT, the treatments of static electric response properties and of excitation spectra are quite different issues.

Since Kohn–Sham DFT yields the exact charge density, in the limit of the exact exchange-correlation functional, properties (such as polarizabilities) which depend only on the response of the charge density to a static, local, applied field are in principle obtained exactly in Kohn–Sham DFT. In practice, good results have been obtained in the local density approximation (LDA) for static dipole polarizabilities and hyperpolarizabilities of molecules using either the finite field method[9–13] or the coupled Kohn–Sham (CKS) method which has been implemented by Colwell, Murray, Handy, and Amos.[14–16] However these approaches are limited to the treatment of static electric fields.

Unlike the situation for static electric response properties, the treatment of excitations within a time-independent DFT framework presents both formal and practical difficulties. Excitation energies may be obtained via a ΔSCF (Δself-consistent-field) approach involving energy differences between DFT SCF calculations with ground vs. excited state configurations. The formal problem that the second Hohenberg–Kohn theorem (or variant thereof) does not apply to (all) excited states becomes a rather practical problem in the commonly encountered case of spin or spatial multiplets which have the same charge density (to first order) but different energies. The usual *ad hoc* solution[17–19] (see also Sec. 6 of Ref. 4 for a simple example) is to suppose that a simple ΔSCF procedure only applies to those excited states

 0021-9606/96/104(13)/5134/14/$10.00

which are well described by a single-determinant wave function. Other multiplet states are then treated by assuming the wave function to be a symmetry-dictated combination of determinants and finding a first-order expression for the energy in terms of the energies of single-determinant states, together with a minimum number of electron-repulsion integrals when the energies of single-determinant states are not sufficient. This approach becomes more difficult for excited states whose multideterminantal character does not simply arise from symmetry. This procedure has been partially automated[19] and a similar method has been used for estimating oscillator strengths.[20,21] In addition to the problem of formal justification and the need to make assumptions about the form of the excited state wave function, other drawbacks of the method include the occasional need to calculate bielectronic integrals which are not normally present in DFT, the need to converge one or more separate SCF calculations for each excited state, and the problem that symmetry breaking may occur (see, for example, the case of acetylene in Ref. 22) which makes state assignment ambiguous. Even though convergence and symmetry breaking problems may be reduced by using the transition state method[23] to estimate ΔSCF excitation energies, time-independent DFT remains cumbersome for calculating electronic excitation spectra.

The formalism of time-dependent DFT (see Ref. 24 for a review) generalizes Kohn–Sham theory to include the case of a time-dependent, local external potential. A practical computational formulation of time-dependent DFT can be developed using time-dependent response theory. This approach has been used successfully both for atoms and for solids.[25] However, the algorithms involved make essential use of the symmetries inherent to the type of system considered, and thus are not suitable for molecular applications. Previous attempts to extend this approach to the molecular regime have used either the jellium sphere model,[26–30] sphericalized potentials,[31–33] or single-center expansions,[34,35] in order to take advantage of atomic-like algorithms, and thus are of no practical utility for molecular calculations.

We report a general molecular implementation of TD-DFRT, using multicenter Gaussian expansions. Preliminary results using the random phase approximation were given in a previous paper.[5] The present paper treats the fully coupled (i.e. TDLDA) method. The formal equations and the auxiliary function method used, respectively, are summarized in Sections II and IV (see Ref. 4 for a detailed exposition of the method). Sec. IV also contains the results of checks on the numerical method. Sec. III gives the computational details. The results for N_2 are presented and discussed in Sec. V, and Sec. VI concludes.

II. FORMALISM

In this section, we give a brief review of the formulation of TD-DFRT detailed in Ref. 4. The starting point is the time-dependent generalization of Kohn–Sham DFT. (See Ref. 24 for a review of the formal foundations of TD-DFT. A brief summary is also given in Ref. 4.) The true (time-dependent) charge density is the sum of the charge densities of the time-dependent Kohn–Sham orbitals,

$$\rho(\mathbf{r},t)=\sum_{i\sigma} f_{i\sigma}|\psi_{i\sigma}(\mathbf{r},t)|^2, \tag{2.1}$$

where the $f_{i\sigma}$ are the orbital occupation numbers. The orbitals are the solutions of the time-dependent Kohn–Sham equation,

$$\left\{-\frac{1}{2}\nabla^2+v(\mathbf{r},t)+\int\frac{\rho(\mathbf{r}',t)}{|\mathbf{r}-\mathbf{r}'|}\,d\mathbf{r}'+\frac{\delta A_{\mathrm{xc}}[\rho_\uparrow,\rho_\downarrow]}{\delta\rho_\sigma(\mathbf{r},t)}\right\}\psi_i^\sigma(\mathbf{r},t)$$
$$=i\frac{\partial}{\partial t}\,\psi_i^\sigma(\mathbf{r},t), \tag{2.2}$$

where v is the external potential and A_{xc} is an exchange-correlation functional from a stationary action principle. No practical exact form for A_{xc} is known, however it is usual to assume the adiabatic approximation,

$$\frac{\delta A_{\mathrm{xc}}[\rho_\uparrow,\rho_\downarrow]}{\delta\rho_\sigma(\mathbf{r},t)}\approx\frac{\delta E_{\mathrm{xc}}[\rho_\uparrow(t),\rho_\downarrow(t)]}{\delta\rho_\sigma(\mathbf{r},t)}, \tag{2.3}$$

where E_{xc} is the exchange-correlation functional from the time-independent theory. Thus, in the case of an external potential which varies slowly in time, Eq. (2.2) is just the obvious time-dependent analogue of the time-independent Kohn–Sham equation. Note that, whereas A_{xc} is a functional of the full space- and time-dependent density, E_{xc} is a functional only of the space-dependent density at the specified time t. Thus, in the adiabatic approximation, there are no retardation effects because the self-consistent field responds instantaneously to any change in the charge density. The adiabatic approximation is thus formally a low-frequency approximation, but like the local density approximation (LDA) for E_{xc} which was originally derived for charge densities varying slowly in space, the useful range of validity of the adiabatic approximation for real systems can only be determined by actual calculations, and may extend beyond what would be expected on the basis of the formal conditions. We restrict ourselves to the adiabatic approximation throughout the present paper. (See Ref. 4 for a more general formulation of TD-DFRT.)

Consider a system initially in its ground electronic state. The linear response to a perturbation $w(t)$ turned on slowly at some time in the distant past is just given by

$$\delta\rho_\sigma(\mathbf{r},\omega)=\sum_{ij}\psi_{i\sigma}(\mathbf{r})\,\delta P_{ij\sigma}(\omega)\,\psi_{j\sigma}^*(\mathbf{r}), \tag{2.4}$$

where

$$\delta P_{ij\sigma}(\omega)=\frac{f_{j\sigma}-f_{i\sigma}}{\omega-(\epsilon_{i\sigma}-\epsilon_{j\sigma})}\times\left[w_{ij\sigma}(\omega)+\sum_{kl\tau}K_{ij\sigma,kl\tau}\delta P_{kl\tau}(\omega)\right] \tag{2.5}$$

is the response of the Kohn–Sham density matrix in the basis of the unperturbed molecular orbitals. The coupling matrix K

TABLE I. Approximation for the coupling matrix **K**. The LDA is used for the exchange and correlation components.

	SCF response terms included in coupling matrix		
Name	Coulomb	Exchange	Correlation
TDLDAxc[a]	√	√	√
TDLDAx	√	√	
RPA[b]	√		
IPA[c]			

[a]Fully coupled adiabatic approximation.
[b]The density-functional theory "random phase approximation" (not the same as time-dependent Hartree–Fock).
[c]"Independent particle approximation," i.e., complete neglect of coupling.

describes the linear response of the self-consistent field v^{SCF} [the last two terms of the orbital Hamiltonian in Eq. (2.2)] to changes in the charge density,

$$K_{ij\sigma,kl\tau}=\frac{\partial v^{\mathrm{SCF}}_{ij\sigma}}{\partial P_{kl\tau}}=\int\int \psi^*_{i\sigma}(\mathbf{r})\psi_{j\sigma}(\mathbf{r})\ \frac{1}{|\mathbf{r}-\mathbf{r}'|}\times\psi_{k\tau}(\mathbf{r}')\psi^*_{l\tau}(\mathbf{r}')d\mathbf{r}d\mathbf{r}'+\int\int \psi^*_{i\sigma}(\mathbf{r})\psi_{j\sigma}(\mathbf{r})\ \frac{\delta^2 E_{\mathrm{xc}}[\rho_\uparrow,\rho_\downarrow]}{\delta\rho_\sigma(\mathbf{r})\delta\rho_\tau(\mathbf{r}')}\times\psi_{k\tau}(\mathbf{r}')\psi^*_{l\tau}(\mathbf{r}')d\mathbf{r}d\mathbf{r}'. \tag{2.6}$$

Note that the functional derivative is evaluated for the unperturbed charge densities, and $\boldsymbol{K}$ is time-independent as a consequence of the adiabatic approximation [Eq. (2.3)]. Physically, this term acts to screen the electrons from the effect of the external perturbation. The first term in Eq. (2.6) gives the response of the coulomb part of v^{SCF}, while the second term can be further divided into the response of the exchange part and the response of the correlation part of v^{SCF}. Consideration of several approximations (specified in Table I) for *K*, consisting of neglecting one or more of these three terms, allow us to determine the relative importance of these different contributions to the response of v^{SCF}.

A. Dynamic polarizability

We give explicit expressions only for the *xz*-component of the polarizability; the treatment is, of course, general. For the time-dependent, electric perturbation

$$w(\mathbf{r},t)=z\mathscr{E}_z(t), \tag{2.7}$$

where $\mathscr{E}_z(t)$ is the applied field strength, the *xz*-component of the dynamic polarizability can be calculated as

$$\alpha_{xz}(\omega)=-2\sum_{ij\sigma}^{f_{i\sigma}-f_{j\sigma}>0} x_{ji\sigma}(\mathrm{Re}\ \delta P_{ij\sigma})(\omega)/\mathscr{E}_z(\omega), \tag{2.8}$$

where $x_{ji\sigma}$ is the matrix element of $\hat{x}$ in the basis of the unperturbed molecular orbitals. Note that only the real part of the response of the density matrix is needed for present purposes. Solving Eq. (2.5) for $\boldsymbol{\delta P}$ and separating the real and imaginary parts then allows the polarizability to be expressed as

$$\alpha_{xz}(\omega)=2\vec{x}^{\dagger}.\mathscr{S}^{-1/2}\{\boldsymbol{\Omega}-\omega^2\mathbf{1}\}^{-1}.\mathscr{S}^{-1/2}\vec{z}, \tag{2.9}$$

where

$$\mathscr{S}_{ij\sigma,kl\tau}=\frac{\delta_{\sigma,\tau}\delta_{i,k}\delta_{j,l}}{(f_{k\tau}-f_{l\tau})(\epsilon_{l\tau}-\epsilon_{k\tau})}>0 \tag{2.10}$$

and

$$\Omega_{ij\sigma,kl\tau}=\delta_{\sigma,\tau}\delta_{i,k}\delta_{j,l}(\epsilon_{l\tau}-\epsilon_{k\tau})^2+2\sqrt{(f_{i\sigma}-f_{j\sigma})(\epsilon_{j\sigma}-\epsilon_{i\sigma})}\times K_{ij\sigma,kl\tau}\sqrt{(f_{k\tau}-f_{l\tau})(\epsilon_{l\tau}-\epsilon_{k\tau})}. \tag{2.11}$$

B. Excitation spectrum

Equation (2.9) has been deliberately cast in the form of the exact sum-over-states (SOS) formula for the mean dynamic polarizability,

$$\bar{\alpha}(\omega)=\frac{1}{3}\,\mathrm{tr}\boldsymbol{\alpha}(\omega)=\sum_I\ \frac{f_I}{\omega_I^2-\omega^2}, \tag{2.12}$$

where the

$$\omega_I=E_I-E_0 \tag{2.13}$$

are vertical excitation energies and the

$$f_I=\frac{2}{3}(E_I-E_0)(|\langle\Psi_0|\hat{x}|\Psi_I\rangle|^2+|\langle\Psi_0|\hat{y}|\Psi_I\rangle|^2+|\langle\Psi_0|\hat{z}|\Psi_I\rangle|^2) \tag{2.14}$$

are the corresponding oscillator strengths. A careful comparison of Eqs. (2.9) and (2.12) shows that excitation energies and oscillator strengths can be obtained from TD-DFRT by solving

$$\boldsymbol{\Omega}\vec{F}_I=\omega_I^2\vec{F}_I \tag{2.15}$$

and calculating

$$f_I=\frac{2}{3}(|\vec{x}^{\dagger}.\mathscr{S}^{-1/2}\vec{F}_I|^2+|\vec{y}^{\dagger}.\mathscr{S}^{-1/2}\vec{F}_I|^2+|\vec{z}^{\dagger}.\mathscr{S}^{-1/2}\vec{F}_I|^2)/|\vec{F}_I|^2. \tag{2.16}$$

The above equations bear a marked resemblence to those of the TDHF method (which can in fact be derived in the same manner but beginning from the HF equation). However there are some important differences. The multiplicative nature of the DFT exchange-correlation potential results in the simple diagonal form (2.10) for $\mathscr{S}$ and thus the simple relation (2.11) between $\boldsymbol{\Omega}$ and **K**. In contrast, in TDHF, the corresponding matrix $\mathscr{S}$ is not diagonal and $\boldsymbol{\Omega}$ involves $\mathscr{S}^{-1/2}$, which is not only computationally less efficient but also sometimes presents more serious difficulties, since $\mathscr{S}$ is not necessarily positive definite (in TDHF). (See Ref. 36 pp. 144–148. Note that their matrix $-\mathbf{S}(\mathbf{A}_{11}-\mathbf{B}_{11})^{-1}\mathbf{S}$ is analogous to our matrix $\mathscr{S}$.) The multiplicative nature of v_{xc} also means that TD-DFRT lends itself to auxiliary function techniques which allow four-center integrals to be eliminated (see Sec. IV). Thus TD-DFRT offers significant computational advantages over TDHF. In addition, the TD-DFRT

method becomes exact in the limit of the exact exchange-correlation functional, A_{xc}, whereas TDHF is, of course, inherently approximate.

Naturally, the approximate functionals which are used in practical calculations place limitations on the quality of the results. In particular, the adiabatic approximation limits the description to excited states which can be described, at zero order, as linear combinations of singly-excited determinants, just as in TDHF. This is easy to see, for a closed shell system, just from counting solutions in a finite basis set. Thus, neither TD-DFRT in the adiabatic approximation nor TDHF would be expected to give especially good results for those excitations having substantial two-hole–two-particle (doubly-excited determinant) character. However, in going beyond the adiabatic approximation, the TD-DFRT coupling matrix becomes frequency dependent. In the exact theory, it is precisely the complicated pole structure of $\mathbf{K}$ in the ω-representation which leads to the proper description of complex excitation processes absent in the adiabatic approximation.

Note that the TD-DFRT equations have been derived within a strictly density-functional formalism and no reference has been made to a wave function. However, for purposes of assigning excitations after they have been calculated, it is convenient, if not strictly necessary, to make some *ansatz* concerning the wave function. One assumes that the *ground state* wave function consists of a single determinant, Φ, of Kohn–Sham orbitals, then (assuming linear independence of the molecular orbital products $\{\psi_{i\sigma}(\mathbf{r})\psi_{j\sigma}(\mathbf{r})\}$) the excited state wave function, Ψ_I, is given (in second quantized notation) by

$$\Psi_I = \sum_{ij\sigma}^{f_{i\sigma}-f_{j\sigma}>0} \sqrt{\frac{\epsilon_{j\sigma}-\epsilon_{i\sigma}}{\omega_I}}\, F^I_{ij\sigma}\hat{a}^\dagger_{j\sigma}\hat{a}_{i\sigma}\Phi + \dots . \qquad (2.17)$$

This seems to be a reasonable approach for the qualitative work of assigning state labels, at least for simple closed-shell systems. Notice that a multideterminantal description of the density response and the transition densities has arisen naturally, with coefficients determined from the eigenvectors in Eq. (2.15), independent of the *ansatz* (2.17).

III. COMPUTATIONAL DETAILS

Calculations of the excitations and polarizability (except for finite-field calculations) were carried out using our post-SCF TD-DFRT program deMon-DynaRho. The SCF step (as well as finite field calculations of the static polarizability) was performed using the Gaussian-type orbital (GTO), auxiliary-function based, molecular DFT program deMon-KS.[6–8] The nitrogen ground state experimental equilibrium internuclear distance of 1.0977 Å[37] was used throughout. All calculations used the LDA parametrization of Vosko, Wilk, and Nusair[38] (extensions to other functionals are left for future work), the (4,4;4,4) auxiliary basis set from the deMon basis set library, and the extrafine random grid which consists of 6208 points per nitrogen atom. Convergence criteria for the SCF step were a change in the total energy of less than 10^{-8} hartree and a change in the charge density fitting coefficients of less than 10^{-8} a.u.

Several GTO orbital basis sets were used in the current study. These include the minimal STO-3G basis set,[39] and the double zeta valence plus polarization (DZVP) and triple zeta valence plus polarization (TZVP) basis sets of Godbout *et al.*[40] from the deMon library. Note that *d* functions in deMon are sets of six cartesian functions. Since diffuse polarization functions are necessary for accurate calculations of polarizabilities, we have used the TZVP basis set augmented with the field-induced polarization functions of Zeiss *et al.*[41] as described in Ref. 12 (TZVP+), and the Sadlej basis set (Sadlej) of Ref. 42, 43. We also used the decontracted Sadlej (DSadlej) basis, since loosening all the orbital contractions in the Sadlej basis has been found to give a good Thomas–Reiche–Kuhn sum.[44] The coupled cluster calculations of excitation energies by Ben-Shlomo and Kaldor,[45] with which we compare our results, used the 6-311G basis augmented with one set of *d* orbitals and two sets each of diffuse *s* and *p* orbitals. Thus we used this basis set as well (BK90). Finally we considered a modified version of a basis set used by Jaszuński *et al.*[46] consisting of the 90CGTO basis used in Ref. 47 with the $2p$ orbital decontracted as in Ref. 46 but with the *f* functions deleted since deMon-KS does not yet handle *f* functions. This is our 88CGTO basis. This was supplemented with three diffuse *s* and two diffuse *p* functions used in Ref. 46 to yield our 106CGTO basis.

IV. AUXILIARY FUNCTION IMPLEMENTATION OF TD-DFRT

The computational advantage of DFT over other *ab initio* methods arises partly from the simple manner in which correlation effects can be included and partly from the locality of the exchange-correlation potential. In particular, this locality means that the potential lends itself readily to auxiliary function techniques[48,49] allowing the costly four-center integrals to be replaced by three-center integrals. Thus auxiliary function based DFT SCF programs such as deMon-KS are able to capitalize on the computational advantages of DFT. In order to maintain this advantage in our implementation of TD-DFRT, we extend the auxiliary function treatment to the coupling matrix so that the four-center integrals that arise in the TD-DFRT formalism are also reduced to three-center integrals. This auxiliary function method is described in the present section (see also Ref. 4), after some preliminaries concerning the use of the auxiliary function expansions in the SCF step. Since our auxiliary function implementation of TD-DFRT is consistent with that used in deMon-KS, the results can be checked by comparison of the deMon-DynaRho static polarizabilities with those obtained from deMon-KS using the finite field method. This comparison is shown at the end of the section.

A. SCF calculations

In order to avoid four-center integrals, two sets of auxiliary basis functions are used in deMon-KS, for the treatment of the coulomb and exchange-correlation integrals, re-

spectively. These are subsequently used in deMon-DynaRho to evaluate the coupling matrix. The following discussion is general for any atomic orbital basis $\{\chi_\mu\}$.

The coulomb integrals,

$$\langle \chi_\mu | v_{\text{coul}} | \chi_\nu \rangle = [\chi_\mu \chi_\nu | \rho], \tag{4.1}$$

where the square brackets denote the inner product

$$[f|g] = \int \int f^*(\mathbf{r}) \frac{1}{|\mathbf{r}-\mathbf{r}'|} g(\mathbf{r}') d\mathbf{r} d\mathbf{r}', \tag{4.2}$$

are handled by expanding the charge density in an atom-centered GTO auxiliary basis set,

$$\rho(\mathbf{r}) \cong \tilde{\rho}(\mathbf{r}) = \sum_I g_I^{\text{cd}}(\mathbf{r}) a_I, \tag{4.3}$$

where the tilde has been added to emphasize that, in practice, this expansion is an approximation since the auxiliary basis is incomplete. The use of $\tilde{\rho}$ in place of ρ in Eq. (4.2) eliminates the need to evaluate four-center integrals and reduces the number of coulomb integrals from N^4 to MN^2 where N is the number of orbital and M is the number of auxiliary basis functions. The expansion coefficients a_I are normally obtained by minimizing $[\rho-\tilde{\rho}|\rho-\tilde{\rho}]$ subject to the constraint

$$\int \tilde{\rho}(\mathbf{r}) d\mathbf{r} = n, \tag{4.4}$$

where n is the number of electrons. This leads to

$$a_I = \sum_J (S^{\text{cd}})^{-1}_{I,J} \left([g_I^{\text{cd}}|\rho] - \lambda \int g_I^{\text{cd}}(\mathbf{r}) d\mathbf{r} \right), \tag{4.5}$$

where

$$S^{\text{cd}}_{I,J} = [g_I^{\text{cd}} | g_J^{\text{cd}}] \tag{4.6}$$

is the charge density overlap matrix, and the Lagrange multiplier

$$\lambda = \frac{\Sigma_{I,J} \int g_I^{\text{cd}}(\mathbf{r}) d\mathbf{r} (S^{\text{cd}})^{-1}_{I,J} [g_J^{\text{cd}}|\rho] - n}{\Sigma_{I,J} \int g_I^{\text{cd}}(\mathbf{r}) d\mathbf{r} (S^{\text{cd}})^{-1}_{I,J} \int g_J^{\text{cd}}(\mathbf{r}') d\mathbf{r}'}. \tag{4.7}$$

It is worth emphasizing that this Lagrange multiplier results from the charge density constraint (4.4) which is believed to be helpful, at least in the case of modest auxiliary basis sets. Without the constraint, $\tilde{\rho}$ is simply the projection of ρ onto the space spanned by the auxiliary basis set and may integrate to a total charge slightly different from n. However, in the limit of a complete charge density auxiliary basis set, $\lambda = 0$ and minor differences in fitting philosophy become irrelevant.

We compared finite field calculations of the static polarizability with (i.e. $\lambda \neq 0$) and without (i.e. setting $\lambda = 0$) the charge density normalization constraint. As shown in Table II, the effect of the charge density normalization constraint on the calculated polarizability of N_2 is insignificant, with the charge density auxiliary baisis set used here. We have found a similar insensitivity of the polarizability to the presence or absence of this constraint in other molecules as well, using the same quality auxiliary basis set.

TABLE II. Comparison of numerical methods for calculation of the mean static polarizability. TZVP+ basis set.

Method	Mean static polarizability (a.u.) Constrained fit[a]	Unconstrained fit[b]
Finite field	11.9469	11.9466
TDLDAxc	11.9332	11.9330
TDLDAxc (SOS)[c]	11.9215	11.9212

[a]Normalization constraint during charge density fit enforced during SCF steps.
[b]No normalization constraint during charge density fit.
[c]Calculation of the oscillator strength sum S_{-2} from the TDLDAxc excitation spectrum.

Thus, since the auxiliary function treatment of the TD-DFRT coupling matrix is simpler in the absence of the charge density normalization constraint, we proceed without using this constraint. For the sake of strict consistency, all the SCF calculations in the rest of this paper are therefore also done without this constraint (i.e. setting $\lambda = 0$). Thus, we calculate the coulomb matrix elements as

$$v^{\text{coul}}_{\mu\nu\sigma} = \sum_{IJ} [\chi_\mu \chi^*_\nu | g_I^{\text{cd}}] \times (S^{\text{cd}})^{-1}_{I,J} \sum_{\mu',\nu',\sigma'} [g_J^{\text{cd}} | \chi_{\mu'} \chi^*_{\nu'}] P_{\mu'\nu'\sigma'}. \tag{4.8}$$

A second auxiliary basis set is used to treat the exchange-correlation integrals. The exchange-correlation potential,

$$v^\sigma_{\text{xc}}(\mathbf{r}) = \frac{\delta E_{\text{xc}}[\rho_\uparrow, \rho_\downarrow]}{\delta \rho_\sigma(\mathbf{r})}, \tag{4.9}$$

is expanded in an atom-centered GTO exchange-correlation auxiliary basis set

$$v^\sigma_{\text{xc}}(\mathbf{r}) \cong \tilde{v}^\sigma_{\text{xc}}(\mathbf{r}) = \sum_I g_I^{\text{xc}}(\mathbf{r}) b_I^\sigma, \tag{4.10}$$

where again the tilde is a reminder that, in practice, the auxiliary basis is incomplete and the expansion is thus an approximation to $v^\sigma_{\text{xc}}(\mathbf{r})$. The fitting coefficients are obtained by minimizing $\{v^\sigma_{\text{xc}} - \tilde{v}^\sigma_{\text{xc}} | v^\sigma_{\text{xc}} - \tilde{v}^\sigma_{\text{xc}}\}$, where the inner product

$$\{f|g\} = \sum_i w_i f^*(\mathbf{r}_i) g(\mathbf{r}_i) \tag{4.11}$$

is defined by numerical quadrature, with weights w_i, over a molecular grid. This gives

$$b_I^\sigma = \sum_J (S^{\text{xc}})^{-1}_{I,J} \{g_J^{\text{xc}} | v^\sigma_{\text{xc}}\}, \tag{4.12}$$

where the exchange-correlation overlap matrix

$$S^{\text{xc}}_{I,J} = \{g_I^{\text{xc}} | g_J^{\text{xc}}\}. \tag{4.13}$$

Thus the exchange-correlation integrals become

$$\langle \chi_\mu | \tilde{v}^\sigma_{\rm xc} | \chi_\nu \rangle = \sum_I \langle \chi_\mu | g^{\rm xc}_I | \chi_\nu \rangle b^\sigma_I$$

$$= \sum_{I,J} \langle \chi_\mu | g^{\rm xc}_I | \chi_\nu \rangle (S^{\rm xc})^{-1}_{I,J} \{ g^{\rm xc}_J | v^\sigma_{\rm xc} \}. \tag{4.14}$$

B. Post-SCF calculations

The coupling matrix (2.6) is the sum of a coulomb and an exchange-correlation part,

$$K_{\mu\nu\sigma,\mu'\nu'\sigma'} = K^{\rm coul}_{\mu\nu\sigma,\mu'\nu'\sigma'} + K^{\rm xc}_{\mu\nu\sigma,\mu'\nu'\sigma'}$$

$$= \frac{\partial v^{\rm coul}_{\mu\nu\sigma}}{\partial P_{\mu'\nu'\sigma'}} + \frac{\partial v^{\rm xc}_{\mu\nu\sigma}}{\partial P_{\mu'\nu'\sigma'}}. \tag{4.15}$$

This allows an auxiliary function expression for the coupling matrix, involving only three-center integrals, to be obtained from the auxiliary function expressions (4.8) and (4.14) for the matrix elements of $v^{\rm coul}$ and $v^{\rm xc}$.

Straightforward differentiation gives

$$K^{\rm coul}_{\mu\nu\sigma,\mu'\nu'\sigma'} = \sum_{I,J} [\chi_\mu \chi_\nu | g^{\rm cd}_I] (S^{\rm cd})^{-1}_{I,J} [g^{\rm cd}_J | \chi_{\mu'} \chi_{\nu'}] \tag{4.16}$$

for the coulomb part of the coupling matrix, and

$$K^{\rm xc}_{\mu\nu\sigma,\mu'\nu'\sigma'} = \sum_{I,J} \langle \chi_\mu | g^{\rm xc}_I | \chi_\nu \rangle \times (S^{\rm xc})^{-1}_{I,J} \left\{ g^{\rm xc}_J \left| \frac{\delta v^\sigma_{\rm xc}}{\delta \rho_{\sigma'}} \right| \chi_{\mu'} \chi_{\nu'} \right\} \tag{4.17}$$

for the exchange-correlation part of the coupling matrix, where

$$\left\{ g^{\rm xc}_J \left| \frac{\delta v^\sigma_{\rm xc}}{\delta \rho_{\sigma'}} \right| \chi_{\mu'} \chi_{\nu'} \right\} = \sum_i w_i g^{\rm xc}_I(\mathbf{r}_i) \frac{\delta v^\sigma_{\rm xc}(\mathbf{r}_i)}{\delta \rho_{\sigma'}(\mathbf{r}_i)} \chi_{\mu'}(\mathbf{r}_i) \chi_{\nu'}(\mathbf{r}_i) \tag{4.18}$$

in the LDA.

Note that the exchange-correlation part of the coupling matrix, which is formally manifestly symmetric [Eq. (2.6)], becomes slightly asymmetric in Eq. (4.17) due to the introduction of a grid and auxiliary basis set. It is symmetrized before solving the eigenvalue problem Eq. (2.15), to ensure real eigenvalues. Similarly, there is also a slight asymmetry in $K^{\alpha\beta}_{\rm xc}$ which leads to a slight mixing of singlet and triplet symmetry in higher lying states in calculations with some of the basis sets reported here. No symmetrization of the $\alpha\beta$-block is done.

Table II shows a check on the numerics of the method. As expected, the TD-DFRT static mean polarizability is in good agreement with the finite field result. Since **K** is symmetrized (by using only half the matrix elements) only when solving the eigenvalue problem Eq. (2.15), polarizabilities calculated via Eq. (2.9), using Eq. (4.17) for $\mathbf{K}^{\rm xc}$, involve the *un*symmetrized **K** (if the whole matrix is calculated), whereas polarizabilities obtained from the sum-over-states formula by first calculating excitation energies and oscillator strengths involve the symmetrized **K**. At the level of the RPA, **K** is symmetric since $\mathbf{K}^{\rm xc}=0$, and these two ways of calculating the polarizability give the same result. At the TDLDAxc level, the slight loss of symmetry of **K** shows up as a slight difference (about 0.1%) between these two ways of calculating the polarizability.

V. RESULTS AND DISCUSSION

In this first report of a fully coupled (i.e. TDLDA), molecular implementation of TD-DFRT, we focus on N_2 as a case study, and give results both for the dynamic polarizability and for the excitation energies. Some preliminary results, at the RPA level, were given in our previous paper.[5] Nitrogen is an important benchmark molecule for excitations, and one for which experimental results for $\bar{\alpha}(\omega)$ are available. It has a complicated manifold of excited states, many of which have an essential multideterminantal nature.

A. Excitation spectrum

The ground state configuration of N_2 obtained from DFT at the SCF level,

$$(1\sigma_g)^2 (1\sigma_u)^2 (2\sigma_g)^2 (2\sigma_u)^2 (1\pi_u)^4 (3\sigma_g)^2, \tag{5.1}$$

differs from that obtained from HF by the ordering of the $1\pi_u$ and $3\sigma_g$ orbitals, with the DFT ordering corresponding to the experimentally observed order of the outer valence ionization potentials.[50] With the exception of the unoccupied $1\pi_g$ orbital which is bound by the LDA effective potential, the unoccupied orbitals represent continuum orbitals and their ordering depends upon the extent to which a given finite basis set is able to describe the continuum. Orbital energies and assignments are shown in Table III. Since the unoccupied orbitals enter into the TD-DFRT calculations, a few of the lowest unoccupied orbitals are included in the table (no unoccupied orbitals are neglected in the actual calculations).

Table IV shows the TDLDAxc vertical excitation energies for the first eight excited states of N_2, calculated with several basis sets. These excitation energies are relatively insensitive to the choice of basis set, the differences across all eight DZVP and larger basis sets never being more than 0.13 eV. If only basis sets including diffuse functions are considered (52 CGTO and larger) the maximum difference reduces to 0.08 eV, and the three largest basis sets agree to within 0.02 eV.

Table V shows the TD-DFRT excitation energies for the first eight excited states, at the IPA, RPA, TDLDAx, and TDLDAxc levels of approximation, in comparison with experiment. (Oscillator strengths are not shown since these are all ''dark'' states.)

The contributions of the response of the coulomb, exchange, and correlation parts of the self-consistent field $v^{\rm SCF}$ can be interpreted in terms of the approximate expressions[4] for the singlet → singlet,

TABLE III. LDA orbital energies for various basis sets.

Orbital	Orbital energies (eV) STO-3G [2s1p]	DZVP [3s2p1d]	TZVP [4s3p1d]	TZVP+ [5s3p2d]	Sadlej [5s3p2d]
Basic size[a]	16	30	38	52	52
Energy (hartree)[b]	−107.147 180	−108.660 889	−108.676 122	−108.680 665	−108.664 712
		Unoccupied orbitals			
$4\sigma_u$		18.26	16.45	5.48	5.76
$2\pi_g$		13.32	9.48	4.49	3.89
$5\sigma_g$		13.12	11.24	4.04	3.20
$2\pi_u$		9.62	6.02	5.49	1.93
$4\sigma_g$		10.04	7.20	0.37	0.66
$3\sigma_u$	19.26	6.37	4.83	1.13	1.35
$1\pi_g$	0.17	−2.05	−2.10	−2.23	−2.23
		Occupied orbitals			
$3\sigma_g$	−7.64	−10.20	−10.23	−10.44	−10.38
$1\pi_u$	−10.56	−11.80	−11.82	−11.94	−11.86
$2\sigma_u$	−11.45	−13.24	−13.24	−13.40	−13.44
$2\sigma_g$	−28.32	−28.34	−28.39	−28.52	−28.37
$1\sigma_u$	−375.96	−380.34	−379.99	−380.18	−380.78
$1\sigma_g$	−375.94	−380.37	−380.03	−380.22	−380.82

Orbital	Orbital energies (eV) BK90 [6s5p1d]	88CGTO [8s6p3d]	DSadlej [10s6p4d]	106CGTO [11s8p3d]
Basis size[a]	54	88	104	106
Energy (hartree)[b]	−108.680 313	−108.695 385	−108.687 781	−108.695 714
		Unoccupied orbitals		
$4\sigma_u$	1.44	11.72	4.38	0.95
$2\pi_g$	1.12	7.06	3.49	1.31
$5\sigma_g$	1.03	5.43	2.72	0.83
$2\pi_u$	0.56	4.06	1.85	0.64
$4\sigma_g$	0.06	3.18	0.45	−0.01
$3\sigma_u$	0.51	3.10	1.05	0.31
$1\pi_g$	−2.29	−2.20	−2.22	−2.22
		Occupied orbitals		
$3\sigma_g$	−10.47	−10.43	−10.46	−10.45
$1\pi_u$	−11.96	−11.87	−11.89	−11.88
$2\sigma_u$	−13.47	−13.43	−13.45	−13.44
$2\sigma_g$	−28.51	−28.31	−28.36	−28.33
$1\sigma_u$	−380.11	−380.02	−380.10	−380.04
$1\sigma_g$	−380.15	−380.06	−380.14	−380.08

[a]Number of contracted Gaussian-type orbitals for N_2.
[b]de Mon-KS "numerical energy."

$$\omega_S \cong \epsilon_a - \epsilon_i + K_{ia\uparrow,ia\uparrow} + K_{ia\uparrow,ia\downarrow}$$
$$= \epsilon_a - \epsilon_i + 2[\psi_i\psi_a|\psi_i\psi_a] + \int \psi_i(\mathbf{r})\psi_a(\mathbf{r})\left[\frac{\delta v_{\mathrm{xc}}^{\uparrow}(\mathbf{r})}{\delta\rho_{\uparrow}(\mathbf{r})} + \frac{\delta v_{\mathrm{xc}}^{\uparrow}(\mathbf{r})}{\delta\rho_{\downarrow}(\mathbf{r})}\right] \times \psi_i(\mathbf{r})\psi_a(\mathbf{r})d\mathbf{r}, \quad (5.2)$$

and singlet → triplet,

$$\omega_T \cong \epsilon_a - \epsilon_i + K_{ia\uparrow,ia\uparrow} - K_{ia\uparrow,ia\downarrow}$$
$$= \epsilon_a - \epsilon_i + \int \psi_i(\mathbf{r})\psi_a(\mathbf{r}) \times \left[\frac{\delta v_{\mathrm{xc}}^{\uparrow}(\mathbf{r})}{\delta\rho_{\uparrow}(\mathbf{r})} - \frac{\delta v_{\mathrm{xc}}^{\uparrow}(\mathbf{r})}{\delta\rho_{\downarrow}(\mathbf{r})}\right]\psi_i(\mathbf{r})\psi_a(\mathbf{r})d\mathbf{r}, \quad (5.3)$$

excitation energies, for excitation from an occupied orbital ψ_i to an unoccupied orbital ψ_a, in a two-state model. (Note that the approximate expression for the singlet → singlet excitation energy given here provides support for the *ansätze* used in the sum-over-states density-functional perturbation theory (SOS-DFPT) of nuclear magnetic resonance chemical shifts,[51] in so far as only exchange and exchange-correlation, but no coulomb, integrals appear.) (Note the resemblence to the well-known corresponding expressions for the Hartree–Fock case.) The IPA excitation energy is just the simple orbital energy difference. For the singlet transitions, this is lower than the TDLDAxc result. Inclusion of the response of the coulomb part of v^{SCF} leads to the exchange integral $[\psi_i\psi_a|\psi_i\psi_a]$ in Eq. (5.2), which increases the excitation energy and gives an RPA value higher than the TDLDAxc

TABLE IV. TDLDAxc vertical excitation energies for the first eight excited states of N_2 calculated with various basis sets.

State	Dominant excitation	STO-3G [2s1p]	DZVP [3s2p1d]	TZVP [4s3p1d]	TZVP+ [5s3p2d]	BK90 [6s5p1d]	Sadlej [5s3p2d]	DSadlej [10s6p4d]	88CGTO [8s6p3d]	106CGTO [11s8p3d]	Expt[a]
					Excitation energy (eV)						
					Singlet→singlet transitions						
$w^1\Delta_u$	$1\pi_u\rightarrow 1\pi_g$	11.56	10.33	10.30	10.28	10.24	10.20	10.22	10.24	10.22	10.27
$a'^1\Sigma_u^-$	$1\pi_u\rightarrow 1\pi_g$	10.74	9.74	9.72	9.70	9.68	9.63	9.66	9.68	9.66	9.92
$a^1\Pi_g$	$3\sigma_g\rightarrow 1\pi_g$	9.03	9.07	9.05	9.11	9.09	9.04	9.10	9.12	9.10	9.31
					Singlet→triplet transitions						
$C^3\Pi_u$	$2\sigma_u\rightarrow 1\pi_g$	10.77	10.35	10.32	10.33	10.34	10.36	10.38	10.39	10.36	11.19
$B'^3\Sigma_u^-$	$1\pi_u\rightarrow 1\pi_g$	10.74	9.74	9.74	9.70	9.68	9.63	9.66	9.68	9.66	9.67
$W^3\Delta_u$	$1\pi_u\rightarrow 1\pi_g$	9.76	8.90	8.90	8.87	8.85	8.80	8.84	8.84	8.83	8.88
$B^3\Pi_g$	$3\sigma_g\rightarrow 1\pi_g$	7.16	7.49	7.51	7.58	7.57	7.53	7.60	7.60	7.60	8.04
$A^3\Sigma_u^+$	$1\pi_u\rightarrow 1\pi_g$	8.63	7.95	7.94	7.91	7.88	7.84	7.88	7.89	7.88	7.75
					Average error for all eight states						
		0.82	0.27	0.27	0.24	0.25	0.27	0.24	0.24	0.25	

[a]Computed in Ref. 53 from the spectroscopic constants of Huber and Herzberg (Ref. 65).

value. The response of the exchange part of v^{SCF} (which contributes only to $\delta v_{\mathrm{xc}}^{\uparrow}/\delta\rho_{\uparrow}$ but not to $\delta v_{\mathrm{xc}}^{\uparrow}/\delta\rho_{\downarrow}$) is negative, thus correcting the RPA value and bringing the TDLDAx closer to the final TDLDAxc value. Inclusion of the response of the correlation part of v^{SCF} is insignificant for the singlets. In contrast, for the triplets, the large term resulting from the response of the coulomb potential cancels out, so the correction to the simple orbital energy difference is due entirely to the response of the exchange-correlation potential. The response of the exchange part reduces the excitation energies, just as for the singlets, but the response of the correlation part is larger for the triplets than for the singlets, and acts to increase the excitation energies. Figure 1 shows the successive splitting of the $\pi\rightarrow\pi^*$ excitations at the different levels of approximation for the coupling matrix.

An important aspect of the TD-DFRT method is that it provides a natural way to handle excitation energies involving excited state multiplets. This is an important aspect of the more general multiplet problem in DFT. In the present context, the problem arises when an excited state requires two or more determinants for its description. The simplest example of this is the splitting of degenerate singly-excited configurations into a singlet,

$$\Psi_0^1=\frac{1}{\sqrt{2}}\,(|\psi_i\bar{\psi}_a|+|\psi_a\bar{\psi}_i|), \tag{5.4}$$

and three degenerate triplet excited states,

$$\Psi_1^3=|\psi_i\psi_a|, \tag{5.5}$$

$$\Psi_0^3=\frac{1}{\sqrt{2}}\,(|\psi_i\bar{\psi}_a|-|\psi_a\bar{\psi}_i|), \tag{5.6}$$

$$\Psi_{-1}^3=|\bar{\psi}_i\bar{\psi}_a|, \tag{5.7}$$

when spin is taken into account. (Spectator orbitals have been neglected for notational convenience.) Although the energy of the triplet can be obtained as the energy of one of the single determinant states, the singlet requires (at least) two determinants. The $\pi\rightarrow\pi^*$ excitations in N_2 (Fig. 1) provide an even more dramatic example of the multiplet problem. This *spatial* multiplet arises from coupling between the x- and y-components of the π orbitals, which gives three distinct *many-electron* symmetries,

$$\Sigma_u^+ : |1\pi_g^x 1\pi_u^y 1\bar{\pi}_u^x 1\bar{\pi}_u^y| + |1\pi_u^x 1\pi_g^y 1\bar{\pi}_u^x 1\bar{\pi}_u^y|$$

TABLE V. Excitation energies for the lowest eight transitions calculated with the Sadlej basis set at the IPA, RPA, TDLDAx, and TDLDAxc levels.

State	Excitation	IPA	RPA	TDLDAx	TDLDAxc	Expt[a]
			Excitation energy (eV)			
			Singlet→singlet transitions			
$w^1\Delta_u$	$1\pi_u\rightarrow 1\pi_g$	9.63	10.94	10.24	10.20	10.27
$a'^1\Sigma_u^-$	$1\pi_u\rightarrow 1\pi_g$	9.63	9.63	9.63	9.63	9.92
$a^1\Pi_g$	$3\sigma_g\rightarrow 1\pi_g$	8.16	9.53	9.07	9.04	9.31
			Singlet→triplet transitions			
$C^3\Pi_u$	$2\sigma_u\rightarrow 1\pi_g$	11.21	11.21	10.09	10.36	11.19
$B'^3\Sigma_u^-$	$1\pi_u\rightarrow 1\pi_g$	9.63	9.63	9.63	9.63	9.67
$W^3\Delta_u$	$1\pi_u\rightarrow 1\pi_g$	9.63	9.63	8.55	8.80	8.88
$B^3\Pi_g$	$3\sigma_g\rightarrow 1\pi_g$	8.16	8.16	7.33	7.53	8.04
$A^3\Sigma_u^+$	$1\pi_u\rightarrow 1\pi_g$	9.63	9.63	7.27	7.84	7.75

[a]Computed in Ref. 53 from the spectroscopic constants of Huber and Herzberg (Ref. 65).

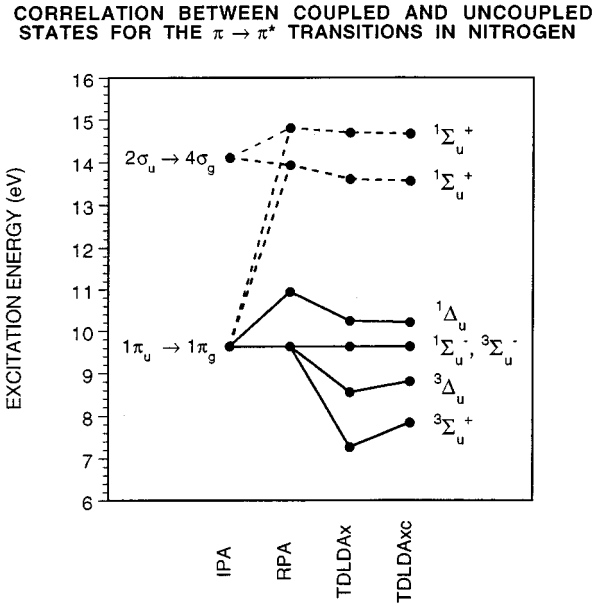

FIG. 1. Correlation between coupled and uncoupled states for the $\pi \rightarrow \pi^*$ transitions in nitrogen. (Sadlej basis set.)

$$\Sigma_u^- : |1\pi_g^y 1\pi_u^y 1\bar{\pi}_u^x 1\bar{\pi}_u^y| - |1\pi_u^x 1\pi_g^x 1\bar{\pi}_u^x 1\bar{\pi}_u^y|$$

$$\Delta_u : |1\pi_g^x 1\pi_u^y 1\bar{\pi}_u^x 1\bar{\pi}_u^y| - |1\pi_u^x 1\pi_g^y 1\bar{\pi}_u^x 1\bar{\pi}_u^y|,$$

$$|1\pi_g^y 1\pi_u^y 1\bar{\pi}_u^x 1\bar{\pi}_u^y| + |1\pi_u^x 1\pi_g^x 1\bar{\pi}_u^x 1\bar{\pi}_u^y|, \qquad (5.8)$$

before spin symmetrization. Spin symmetrization yields a total of eight multideterminantal states (including two pairs of states degenerate by symmetry), requiring linear combinations of (at least) four determinants each. However the correct multideterminantal description of spin and spatial multiplets is obtained automatically in TD-DFRT, with the wave function *ansatz* of Eq. (2.17), since the eigenvectors of $\mathbf{\Omega}$ [Eq. (2.15)] give the coefficients of the various determinants [Eq. (2.17)]. Recall that the multiplet splittings and assignments of spin multiplicity in TD-DFRT do not depend on the wave function *ansatz* (2.17) which is used here only to enable a discussion of the wave function concept of a multideterminantal description. This multideterminantal description of excited states in TD-DFRT is, of course, not limited to multiplets arising from symmetry, but includes the mixing of configurations more generally. An example of the latter is seen in the case of the $^1\Sigma_u^+$ state in Fig. 1. Although the other transitions shown are primarily symmetry-determined combinations of $1\pi_u \rightarrow 1\pi_g$ excitations, the $^1\Sigma_u^+$ state mixes strongly, so that there is no $^1\Sigma_u^+$ state which arises predominantly from the zero-order $1\pi_u \rightarrow 1\pi_g$ excitation. (This was also found in the MRCCSD calculation of Ben-Shlomo and Kaldor.[45]) A less dramatic example of configuration mixing in the TDLDAxc is the lowest $^3\Sigma_u^+$ state which, although predominantly $1\pi_u \rightarrow 1\pi_g$ also has small $\sigma_g \rightarrow \sigma_u$ and $\sigma_u \rightarrow \sigma_g$ contributions. The multideterminantal treatment of excited states in TD-DFRT is, of course, completely analogous to TDHF. In many cases this is sufficient to remove the worst difficulties associated with the multiplet problem in the DFT treatment of molecular excitations.

Overall, the TDLDAxc results are in quite good agreement with experiment, with an average absolute error, for these lowest states, of about 0.25 eV. Only two transitions have an error larger than 0.3 eV, namely those to the $C^3\Pi_u$, with an error of 0.83 eV, and the $B^3\Pi_g$, with an error of about half an eV. This relatively large error in the $B^3\Pi_g$ transition energy compared to that of the $A^3\Sigma_u^+$ leads to an inverted ordering of these two energetically similar states. One might suspect that the larger errors for these triplets might arise because the orbitals are determined for a singlet (the ground state). Since one of the three degenerate $B^3\Pi_g$ is well represented by a single determinant, and is the lowest state of its symmetry, this can be checked. The ΔSCF method is straightforward for this state. A DFT SCF calculation constrained to triplet multiplicity (i.e. $M_s=1$) finds the lowest state to be of $^3\Pi_g$ symmetry, at an energy of 7.59 eV above the ground state, using the Sadlej basis set (as compared to 7.53 eV from TDLDAxc with the same basis.) Thus, in this case, ΔSCF suffers from the same magnitude of error and inverted ordering of states as TDLDAxc, suggesting that the problem is with the LDA functional. However it should be kept in mind that the energies of the $A^3\Sigma_u^+$ and $B^3\Pi_g$ states are very close at the ground-state equilibrium geometry, and an exploration of the potential energy curves is certainly warranted to see if the incorrect ordering persists for other bond distances.

Table VI shows the TDLDAxc results in comparison with results from other *ab initio* methods. Although the other theoretical results, taken from the literature, were obtained with various different basis sets, this should not seriously affect the comparison, since the excitation energies of these states are not terribly sensitive to quality of basis sets of at least double zeta plus polarization quality. This was noted above for the TDLDAxc results, and there is a similar agreement between the other theoretical values shown in Table VI (from Refs. 45, 46, 52, 53) and corresponding values obtained using other basis sets (from Refs. 1, 52).

The average error in the TDLDAxc results, for the first eight states, is comparable to that for the multiconfigurational time-dependent Hartree–Fock (MCTDHF) results. The TD-DFRT formalism is closely analogous to that of TDHF. However, TDHF is notoriously unreliable for triplet excitation energies.[1,54] This is especially true in the case of a ''triplet instability'' (i.e. when the SCF reference wave function is unstable with respect to symmetry breaking[55]), since the TDHF excitation energy may then be imaginary (Ref. 36 pp. 147–8). The TDHF results for the singlets are not particularly good either, with an average error of 1.3 eV for the first three singlets in N_2. The problem of triplet instabilities, or near instabilities, in TDHF is a reflection of inadequacies of the reference wave function. This problem is rectified in MCTDHF by the use of a multideterminantal reference state. One might hope also to avoid the problem of instabilities in TD-DFRT if the functional includes a sufficient description of ground state correlation. This does seem to be the case for

TABLE VI. Comparison of TDLDAxc vertical excitation energies for the first eight excited states of N_2 with experiment and with other *ab initio* results. $R_{NN}=2.074$ bohr.

State	Excitation	Excitation energy (eV) TDLDAxc[a]	Expt[b]	MRCCSD[c]	SOPPA[d]	MCTDHF[d]	TDHF[g]	TDA[h]
Singlet→singlet transitions								
$w^1\Delta_u$	$1\pi_u\rightarrow 1\pi_g$	10.22	10.27	10.54	10.51	10.76	8.75	9.09
$a'^1\Sigma_u^-$	$1\pi_u\rightarrow 1\pi_g$	9.66	9.92	10.09	10.02	10.40	7.94	8.51
$a^1\Pi_g$	$3\sigma_g\rightarrow 1\pi_g$	9.10	9.31	9.28	9.32	9.60	9.76	9.60
Singlet→triplet transitions								
$C^3\Pi_u$	$2\sigma_u\rightarrow 1\pi_g$	10.36	11.19	11.19	11.05	11.43	11.26	11.85[i]
$B'^3\Sigma_u^-$	$1\pi_u\rightarrow 1\pi_g$	9.66	9.67	9.87	9.96	10.07	7.94	8.51
$W^3\Delta_u$	$1\pi_u\rightarrow 1\pi_g$	8.83	8.88	8.93	8.93	8.86	5.80	7.35
$B^3\Pi_g$	$3\sigma_g\rightarrow 1\pi_g$	7.60	8.04	8.05	7.87	8.17	7.62	7.94
$A^3\Sigma_u^+$	$1\pi_u\rightarrow 1\pi_g$	7.88	7.75	7.56	7.91[a]	7.64	3.47	6.25
Average error for all eight states								
		0.25		0.11	0.14	0.27	1.69	1.02

[a]106CGTO basis.
[b]Computed in Ref. 53 from the spectroscopic constants of Huber and Herzberg (Ref. 65).
[c]Multireference coupled cluster singles and doubles, BK90 basis set (52 CGTO), Ref. 45.
[d]Second-order polarization propagator approximation, 58 CGTO basis set, $R_{NN}=2.068$ bohr, Ref. 53.
[e]36 CGTO basis set, may differ significantly from 58CGTO result.
[f]Multiconfigurational time-dependent Hartree–Fock, $[11s8p4d1f]$ basis set, Ref. 46.
[g]Time-dependent Hartree–Fock, $[11s8p4d1f]$ basis set, Ref. 46.
[h]Tamm–Dancoff approximation, DZP (30 CGTO) basis, Ref. 52.
[i]66 CGTO basis, $R_{NN}=2.067$ bohr, Ref. 1; the four other values available from this calculation differ from the ones shown here by $\leqslant 0.07$ eV.

N_2 where we found no particular problem with triplet excitation energies. (It is also interesting to note that in TDDFRT calculations on Na_4, instabilities did occur when correlation was neglected both at the SCF and TDLDAx levels, but did not occur when correlaton was included at the SCF level and the TDLDAxc was used.[56]) The Tamm–Dancoff approximation (TDA), also known as singles configuration-interaction (CIS), starts with the HF ground state, as does TDHF, but the TDA gives a more approximate description of the excitation operator than does TDHF. (In the equations of motion formalism, $[\mathbf{H},\mathcal{O}]=\omega\mathcal{O}$ is solved for the excitation operator $\mathcal{O}$, which is expanded in terms of excitation and de-excitation operators in TDHF, but the de-excitation operators are neglected in the TDA.) The TDA does not suffer from triplet instabilities, and gives better excitation energies than does TDHF, though the TDA results are still not particularly good, with an average error of 1.0 eV for the states considered here. It is interesting to note that the close, but non-degenerate, singlet and triplet Σ_u^- states (0.25 eV apart) are degenerate at the TDLDAxc, TDHF, and TDA levels, but this degeneracy is broken in MCTDHF. Thus, this splitting evidently arises from correlation not included in the TDLDAxc. The second order polarization propagator approximation (SOPPA) and multireference coupled cluster singles and doubles (MRCCSD), with average errors of 0.14 and 0.11 eV, respectively, both do better than the TDLDAxc. Note that the major part of the difference in average error between the TDLDAxc and SOPPA or MRCCSD is due to the large error for the $C^3\Pi_u$ state in the TDLDAxc (the TDLDAxc average error for the first *seven* states is 0.16 eV).

Finally, we note that the TDLDAxc excitation energies for the higher states, not reported here, are sensitive to the basis set and are not converged even with the largest basis set used. Two of the basis sets (BK90 and 106CGTO, which contain the smallest exponents) give a marked reduction of the positive orbital energies (see Table III), with a concommittant decrease in the excitation energies for transitions other than those dominated by excitations to the $1\pi_g$ orbital (i.e. for the states higher than the ones reported here). This is consistent with the onset of the ionization continuum occuring at too low an energy in the TDLDA: Although LDA ionization potentials are normally calculated as the difference between the ground state energies of the parent neutral and daughter cation, it can be shown (Ref. 25 pp. 97–98) that ionization occurs in the TDLDA when ω exceeds the negative of the Kohn–Sham HOMO orbital energy. (In particular, it is shown that the asymptotic behavior of the second-order response of the charge density is nondecaying at these energies.) This is not a problem in principle because, in the limit of the exact functional E_{xc}, the negative of the Kohn–Sham HOMO orbital energy can be shown to be equal to the first ionization potential (IP).[57] However, in practice, it is well known that the LDA HOMO energy substantially underestimates the first IP. For N_2, $-\epsilon_{\mathrm{HOMO}}^{\mathrm{LDA}}\cong 10.4$ eV, whereas the first IP is 15.6 eV.[50] In this context, it is interesting to note that the $C^3\Pi_u$ state, for which the error in the TDLDAxc excitation energy is about 0.4 eV larger than for any other state, has an experimental excitation energy significantly above the TDLDA ionization threshold $(-\epsilon_{\mathrm{HOMO}})$.

B. Polarizabilities

The dynamic mean polarizability is related to the excitation spectrum through the Cauchy expansion

TABLE VII. Coefficients (in a.u.) of Cauchy (ω^2) expansion of mean dynamic polarizability at IPA, RPA, TDLDAx, and TDLDAxc levels.

Method	S_0	S_{-2}[a]	S_{-4}	S_{-6}	S_{-8}	S_{-10}	S_{-12}	S_{-14}
				TZVP+ basis set				
IPA	11.48	21.21	111.4	735.3	5256	3.894×10^4	2.941×10^5	2.246×10^6
RPA	11.48	10.78	26.65	85.17	309.7	1.240×10^3	5.355×10^3	2.445×10^4
TDLDAx	11.48	11.81	32.01	110.8	430.1	1.812×10^3	8.123×10^3	3.814×10^4
TDLDAxc	11.48	11.92	32.71	114.5	449.6	1.915×10^3	8.686×10^3	4.133×10^4
				Sadlej basis set				
IPA	10.44	21.56	115.1	769.2	5554	4.158×10^4	3.177×10^5	2.459×10^6
RPA	10.44	10.95	28.42	97.79	382.2	1.610×10^3	7.125×10^3	3.257×10^4
TDLDAx	10.44	12.00	33.99	125.9	523.7	2.325×10^3	1.076×10^4	5.116×10^4
TDLDAxc	10.44	12.11	34.83	131.3	555.5	2.509×10^3	1.180×10^4	5.706×10^4
				Experiment[b]				
	14[c]	11.74	30.11	101.8	384.6	1.534×10^3	6.307×10^3	2.646×10^4

[a]Mean static polarizability.
[b]Reference 66.
[c]Exact value equals number of electrons.

$$\bar{\alpha}(\omega)=\sum_{l=1}^{\infty} S_{-2l}\omega^{2(l-1)}, \tag{5.9}$$

where the coefficients

$$S_{-2l}=\sum_I \omega_I^{-2l} f_I \tag{5.10}$$

are obtained from the SOS formula [Eq. (2.12)]. This expansion is convergent for ω below the first "bright state," (i.e. below the first excitation energy having nonzero oscillator strength), thus below about 13 eV[58] for N_2.

The relative contributions of the response of the coulomb, exchange, and correlation parts of v^{SCF} to the polarizability parallel those noted above for the singlet excitation energies, as is expected from their interrelation through the oscillator sums. Table VII shows the effect on the mean static polarizability, S_{-2}, of these successive contributions to the coupling matrix. It should be remembered that these terms correspond to the *response* of the respective parts of v^{SCF} to the applied field; the complete (LDAxc) v^{SCF} is of course used at the SCF step, so the zero-order orbitals and orbital energies are at the LDAxc level. The TDLDAxc result is in good agreement with experiment, as had been found previously using the finite field method.[12] The IPA, which consists of completely neglecting the response of v^{SCF} to the applied field, gives a result which is twice as large as the experimental value. Including only the coulomb part of the response of v^{SCF} (i.e. the RPA), already gives a much more reasonable value, though it over-corrects. We have observed a similar effect in several other small molecules.[5] This is easy to understand physically. An applied field induces a dipole in the molecule. The induced field resulting from the dipole acts to reduce the net field felt by the electrons in the molecule, hence reducing the polarizability which measures the response of the electrons, not to the local field within the molecule, but to the applied field. In Kohn–Sham DFT, the production of a local field different from the applied field is described by the response of v^{SCF} to the applied field, i.e. by the coupling matrix in TD-DFRT. Thus, completely neglecting the coupling matrix (i.e. IPA) should be expected to give a polarizability which is too large, and the RPA, which includes the response of the coulomb part of v^{SCF}, should basically account for this physical effect. A large part of the effect of the exchange term is to partially correct the well-known self-interaction error in the coulomb term, and the inclusion of the response of the exchange term (TDLDAx) gives a small but significant ($\sim$10%) adjustment to the RPA overcorrection of the polarizability. Including the response of

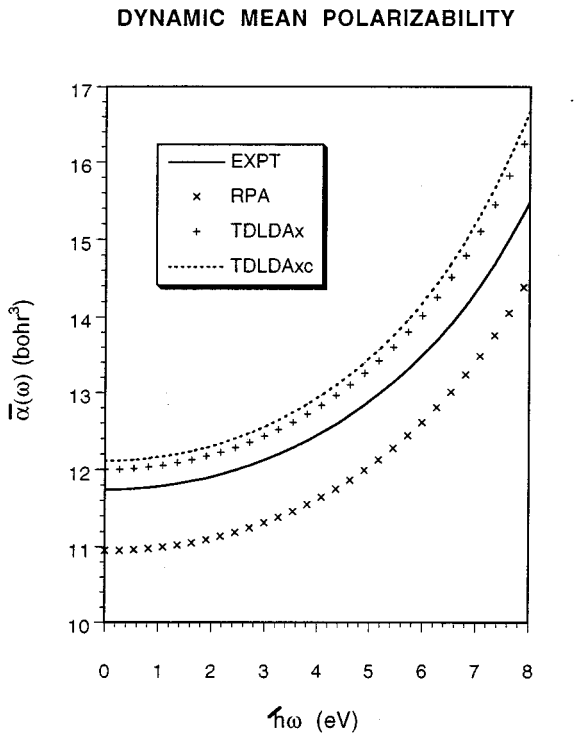

FIG. 2. Comparison of the TD-DFRT dynamic mean polarizability, calculated using the Sadlej basis set, with experiment. Both the theoretical and experimental curves were generated from the Cauchy moments shown in Table VII.

TABLE VIII. Comparison of TDLDAxc Cauchy coefficients (in a.u.) with those from other *ab initio* methods and with experiment. $R_{NN}=2.074$ bohr.

Method	Basis set	S_0	S_{-2}[a]	S_{-4}	S_{-6}
		TD-DFRT Calculations			
TDLDAxc	TZVP+	11.48	11.92	32.71	114.5
	BK90	12.96	10.56	31.93	127.98
	Sadlej	10.44	12.11	34.83	131.3
	DSadlej	13.99	12.19	34.00	128.2
	88CGTO	14.04	11.55	29.32	99.12
	106CGTO	14.03	11.73	31.70	121.1
		Experiment[b]			
		14[c]	11.74	30.11	101.8
		Other theory			
TDHF[d]	$[11s8p4d1f]$	13.96	11.56	27.60	100.51
TDHF[e]	$[7s5p3d]$		11.44	27.53	83.56
TDHF[f]	DSadlej	14.01	11.54	27.39	83.84
MCTDHF[g]	$[11s8p4d1f]$		11.06	25.61	68.53
MCTDHF[h]	$[8s6p4d1f]$			28.92	94.51
SOPPA[i]	DSadlej		11.42	29.24	98.6

[a]Mean static polarizability.
[b]Reference 66.
[c]Exact value equals number of electrons.
[d]Time-dependent Hartree–Fock calculation of Ref. 46.
[e]Time-dependent Hartree–Fock calculation of Ref. 67.
[f]Time-dependent Hartree–Fock calculation of Ref. 44
[g]Multiconfigurational time-dependent Hartree–Fock calculation of Ref. 46. Six orbital active space.
[h]Multiconfigurational time-dependent Hartree–Fock calculation of Ref. 60. Twelve orbital active space.
[i]Second-order polarization propagator approximation calculation of Ref. 44.

the correlation term is relatively unimportant, consistent with the fact that the correlation term is typically only about one tenth of the magnitude of the exchange term in molecules. The small change in $\bar{\alpha}(0)$ in going from TDLDAx to TDLDAxc is not an improvement, though both are in good agreement with experiment.

Figure 2 shows the dynamic mean polarizability at the RPA, TDLDAx, and TDLDAxc levels, in comparison with experiment. (The IPA is too far off to be seen on this graph.) The TDLDAx and TDLDAxc are both in fairly good agreement with experiment. The relative contributions of the different coupling terms are similar to those for the static case. It is interesting to note that the RPA does better for describing the frequency dependence than for $\bar{\alpha}(0)$. That is, if the RPA is used only to describe the frequency dependence $[\bar{\alpha}(\omega)-\bar{\alpha}(0)]$ and this is added to the TDLDAxc value for $\bar{\alpha}(0)$, the resulting shifted curve is a reasonable approximation. This is analogous to the ''additive correction'' method (Ref. 59 p. 8) frequently employed to combine TDHF frequency dependence with correlated $\bar{\alpha}(0)$ values.

The Cauchy moments, S_{-2l}, calculated at the IPA, RPA, TDLDAx, and TDLDAxc levels are shown in Table VII, in comparison with experiment. The Thomas–Reiche–Kuhn (TRK) sum

$$S_0=\sum_I f_I, \tag{5.11}$$

is also included in the table, although it does not enter into the expansion (5.9) of the polarizability. As discussed in Ref. 4, within the adiabatic approximation [Eq. (2.3)] of TD-DFRT, the $\vec{F}_I$ form a complete orthonormal basis set for the space defined by single excitations out of the molecular orbitals from the original finite-basis SCF calculation. Using this completeness and the oscillator strength expression (2.16) then gives

$$\sum_I f_I=\frac{2}{3}\,(\vec{x}^{\dagger}.\mathscr{S}^{-1}\vec{x}+\vec{y}^{\dagger}.\mathscr{S}^{-1}\vec{y}+\vec{z}^{\dagger}.\mathscr{S}^{-1}\vec{z}), \tag{5.12}$$

which depends only on the molecular orbitals and orbital energies from the initial SCF calculation, and thus is the same for all frequency-independent approximations (e.g. IPA, RPA, TDLDAx, TDLDAxc) for the TD-DFRT coupling matrix. This is, of course, exactly what is observed for S_0 in Table VII. Furthermore, since the TRK sum clearly becomes equal to the number of electrons in the IPA, in the limit of a complete one-electron basis set, the TRK sum will also approach the same limit for any TD-DFRT calculation using a frequency-independent coupling matrix. In Table VIII the three largest basis sets give TRK sums quite close to the 14 electron exact value. However, the TRK sum should not be overinterpreted as a measure of the quality of the basis set, since the excitation-energy weightings differ in the different oscillator sums. Note that the Cauchy moments S_{-2} and higher differ significantly between these three basis sets.

The coefficient S_{-4}, while not as good as the mean static polarizability, is still reasonably good. However the quality of the coefficients S_{-2l} deteriorates rapidly as l increases from 1 to 7. This is particularly true of the TDLDAx and TDLDAxc (as opposed to RPA) results. Although the contribution of the response of the exchange-correlation part of v^{SCF} (as a fraction of the TDLDAxc value) increases with l, the response of the coulomb part remains by far the largest

correction to the independent particle approximation. Of course it is only the first few coefficients which make a substantial contribution to the total $\bar{\alpha}(\omega)$.

Obviously it is only the bright states that contribute to the Cauchy coefficients (5.10). In view of the difficulties of calculating these higher energy excitations, it is not surprising that the dynamic polarizability is more sensitive to the basis set than are the low-lying excitation energies. Although the BK90, 88CGTO and 106CGTO basis sets are fine for the low excitations, they are not expected to be adequate for the polarizability due to a lack of diffuse *d* functions. While the DSadlej basis gives a much better TRK sum than the Sadlej basis, the Cauchy moments from these two basis sets are not very different.

Table VIII shows the TDLDAxc oscillator sums in comparison with results from TDHF, MCTDHF, and SOPPA. The several TDHF results shown here for the static polarizability and S_{-4} are all in very good agreement with each other, while S_{-6} seems to be somewhat more sensitive to the basis set. Our DSadlej basis set is the same as that used in Ref. 44. Comparing the values using this basis set, the errors in the TDLDAxc S_{-2}, S_{-4}, and S_{-6} (3.8%, 13%, and 26%, respectively) are somewhat larger than those for TDHF (1.7%, 9.0%, and 18%), and SOPPA does better than TDHF for S_{-4}, and S_{-6}. The MCTDHF results seem to be very similar to those from SOPPA when a large active space is used in the MCTDHF (12-orbital active space in Ref. 60, vs. 6-orbital active space in Ref. 46), though the basis sets used in the two MCTDHF calculations are not the same.

As a result of the onset of the continuum occuring at too low an energy in the LDA, one would expect the energies of the bright states, especially the first several, (all of which lie above the LDA ionization threshold of about 10.4 eV) to be too low. This is generally what we find, though in some cases basis set deficiencies raise (some of) the excitation energies, offsetting this effect. The result is that the TDLDAxc Cauchy moments should be too large, and this should become more pronounced as *l* increases, since the contribution of the lower bright states becomes more predominant for higher *l*. This is indeed what we observe (Table VII). It is also interesting to note that the HF Koopmans' theorem IP for N_2 is too high (16.8 eV[45] compared to the experimental value of 15.6 eV[50]), though the error is smaller than for the LDA, and the TDHF Cauchy moments are too low, the error increasing with *l* but remaining smaller than that for the LDA.

VI. CONCLUSION

A time-dependent molecular density-functional response theory method has been implemented as a post-deMon-KS program deMon-DynaRho which makes possible the DFT calculation of molecular frequency-dependent electric response properties and excitation spectra based on a rigorous time-dependent DFT and response theory formulation. We have demonstrated the viability of extending the use of auxiliary-function techniques (which are common to the more efficient of the Gaussian-orbital-based DFT codes) to the calculation of the coupling matrix, with the result that our TD-DFRT algorithm does not require the evaluation of four-center integrals. The resulting excitation energies for the first eight excited states of N_2 are in good agreement with experiment, and with MRCCSD, SOPPA, and MCTDHF results, though for the highest state, which is nearly at the LDA ionization threshold, the TDLDAxc excitation energy has a substantially higher error than for the other states. Nevertheless, the TDLDAxc excitation energies for the states considered here are much better than those given by TDHF or by the Tamm–Dancoff approximation (also known as CIS), and no difficulties with singlet-triplet excitation energies (as occur in TDHF) were found. The TDLDAxc dynamic mean polarizability of N_2 is also in fairly good agreement with experiment, though the quality of the higher Cauchy moments deteriorates rapidly with increasing order. This, as well as the difficulties with high-lying excited states, is consistent with the well-known problem that the LDA substantially underestimates the ionization threshold. Thus the use of self-interaction corrections, or of recent functionals for v_{xc},[61–64] which largely correct this problem, may be expected to improve the high-lying excitations and Cauchy moments. In view of the generally good quality of these first results for N_2, especially for the low-lying excitations, studies of a variety of molecules are clearly needed, in order to assess the performance of TD-DFRT, both at the LDA level and using improved functionals.

ACKNOWLEDGMENTS

We would like to thank Normand Desmarais for use of his code management program MkProj, Vladimir Malkin and Olga Malkina for interesting discussions concerning the relation between TD-DFRT and the SOS-DFPT of Ref. 51 and Kim Casida for comments on a draft of this manuscript. Financial support through grants from the Natural Sciences and Engineering Research Council (NSERC) of Canada, the Canadian Centre of Excellence in Molecular and Interfacial Dynamics (CEMAID), and the Fonds pour la formation des chercheurs et l'aide à la recherche (FCAR) of Québec is gratefully acknowledged.

[1] J. Oddershede, Adv. Chem. Phys. **69**, 201 (1987).
[2] J. E. Rice and N. C. Handy, J. Chem. Phys. **94**, 4959 (1991).
[3] J. E. Rice and N. C. Handy, Int. J. Quantum Chem. **43**, 91 (1992).
[4] M. E. Casida, in *Recent Advances in Density-Functional Methods*, edited by D. P. Chong (World Scientific, Singapore, in press).
[5] M. E. Casida, C. Jamorski, F. Bohr, J. Guan, and D. R. Salahub, in *Theoretical and Computational Modeling of NLO and Electric Materials*, edited by S. P. Karna and A. T. Yeates (ACS, Washington, D.C., in press).
[6] A. St-Amant and D. R. Salahub, Chem. Phys. Lett. **169**, 387 (1990).
[7] A. St-Amant, Ph.D. thesis, Université de Montréal, 1992.
[8] D. R. Salahub, M. Castro, and E. I. Proynov, in *Relativistic and Electron Correlation Effects in Molecules and Solids*, edited by G. L. Malli, Vol. 318, *Nato Advanced Study Institute, Series B: Physics* (Plenum, New York, 1994).
[9] P. G. Jasien and G. Fitzgerald, J. Chem. Phys. **93**, 2554 (1990).
[10] F. Sim, D. R. Salahub, and S. Chin, Int. J. Quantum Chem. **43**, 463 (1992).
[11] D. P. Chong, J. Chin. Chem. Soc. **39**, 375 (1992).
[12] J. Guan, P. Duffy, J. T. Carter, D. P. Chong, K. C. Casida, M. E. Casida, and M. Wrinn, J. Chem. Phys. **98**, 4753 (1993).
[13] J. Guan, M. E. Casida, A. Köster, and D. R. Salahub, Phys. Rev. B **52**, 2184 (1995).

[14] S. M. Colwell, C. W. Murray, N. C. Handy, and R. D. Amos, Chem. Phys. Lett. **210**, 261 (1993).
[15] A. M. Lee and S. M. Colwell, J. Chem. Phys. **101**, 9704 (1994).
[16] S. A. C. McDowell, R. D. Amos, and N. C. Handy, Chem. Phys. Lett. **235**, 1 (1995).
[17] R. P. Messmer and D. R. Salahub, J. Chem. Phys. **65**, 779 (1976).
[18] T. Ziegler, A. Rauk, and E. J. Baerends, Theor. Chim. Acta **43**, 877 (1977).
[19] C. Daul, Int. J. Quantum Chem. **52**, 867 (1994).
[20] F. Rogemond, H. Chermette, and D. R. Salahub, Chem. Phys. Lett. **219**, 228 (1994).
[21] G. Gardet, F. Rogemond, and H. Chermette, Theor. Chim. Acta **91**, 249 (1995).
[22] P. Duffy, D. P. Chong, M. E. Casida, and D. R. Salahub, Phys. Rev. A **50**, 4707 (1994).
[23] J. C. Slater, Adv. Quantum Chem. **6**, 1 (1972).
[24] E. K. U. Gross and W. Kohn, Adv. Quantum Chem. **21**, 255 (1990).
[25] G. D. Mahan and K. R. Subbaswamy, *Local Density Theory of Polarizability* (Plenum, New York, 1990).
[26] D. E. Beck, Phys. Rev. B **30**, 6935 (1984).
[27] M. J. Puska, R. M. Nieminen, and M. Manninen, Phys. Rev. B **31**, 3486 (1985).
[28] M. Manninen, R. M. Nieminen, and M. J. Puska, Phys. Rev. B **33**, 4289 (1986).
[29] P. Stampfli and K. H. Bennemann, Phys. Rev. A **39**, 1007 (1989).
[30] G. Bertsch, Comput. Phys. Commun. **60**, 247 (1990).
[31] A. Rubio, L. C. Balbás, and J. A. Alonso, Phys. Rev. B **45**, 13657 (1992).
[32] A. Rubio, L. C. Balbás, and J. A. Alonso, Phys. Rev. B **46**, 4891 (1992).
[33] L. C. Balbás, A. Rubio, and M. B. Torres, Computat. Mat. Sci. **2**, 509 (1994).
[34] Z. H. Levine and P. Soven, Phys. Rev. Lett. **50**, 2074 (1983).
[35] Z. H. Levine and P. Soven, Phys. Rev. A **29**, 625 (1984).
[36] P. Jørgensen and J. Simons, *Second Quantization-Based Methods in Quantum Chemistry* (Academic, New York, 1981).
[37] K. P. Huber and G. Herzberg, *Molecular Spectra and Molecular Structure. IV. Constants of Diatomic Molecules* (Van Nostrand Reinhold, New York, 1979), pp. 412–425.
[38] S. H. Vosko, L. Wilk, and M. Nusair, Can. J. Phys. **58**, 1200 (1980).
[39] W. J. Hehre, R. F. Stewart, and J. A. Pople, J. Chem. Phys. **51**, 2657 (1969).
[40] N. Godbout, D. R. Salahub, J. Andzelm, and E. Wimmer, Can. J. Chem. **70**, 560 (1992).
[41] G. D. Zeiss, W. R. Scott, N. Suzuki, D. P. Chong, and S. R. Langhoff, Mol. Phys. **37**, 1543 (1979).
[42] A. J. Sadlej, Theor. Chim. Acta **79**, 123 (1991).
[43] A. J. Sadlej, Coll. Czech. Chem. Commun **53**, 1995 (1988).
[44] M. J. Packer, S. P. A. Sauer, and J. Oddershede J. Chem. Phys. **100**, 8969 (1994)
[45] U. Kaldor and S. B. Ben-Shlomo, J. Chem. Phys. **92**, 3680 (1990).
[46] M. Jaszunski, A. Rizzo, and D. L. Yeager, Chem. Phys. **136**, 385 (1989).
[47] A. Rizzo, R. L. Graham, and D. L. Yeager, J. Chem. Phys. **89**, 1533 (1988).
[48] H. Sambe and R. H. Felton, J. Chem. Phys. **62**, 1122 (1975).
[49] B. I. Dunlap, J. W. D. Connolly, and J. R. Sabin, J. Chem. Phys. **71**, 3396 (1979).
[50] D. W. Turner, C. Baker, A. D. Baker, and C. R. Brundle, *Molecular Photoelectron Spectroscopy* (Wiley, New York, 1970).
[51] V. G. Malkin, O. L. Malkina, M. E. Casida, and D. R. Salahub, J. Am. Chem. Soc. **116**, 5898 (1994).
[52] S. Pal, M. Rittby, R. J. Barlett, D. Sinha, and D. Mukherjee, J. Chem. Phys. **88**, 4357 (1988).
[53] J. Oddershede, N. E. Grüner, and G. H. F. Diercksen, Chem. Phys. **97**, 303 (1985).
[54] P. Jørgensen, Ann. Rev. Phys. Chem. **26**, 359 (1975).
[55] J. Čížek and J. Paldus, J. Chem. Phys. **47**, 3976 (1967).
[56] J. Guan, C. Jamorski, M. E. Casida, and D. R. Salahub (unpublished).
[57] C.-O. Almbladh and U. von Barth, Phys. Rev. **31**, 3231 (1985).
[58] J. Geiger and B. Schröder, J. Chem. Phys. **50**, 7 (1969).
[59] D. P. Shelton and J. E. Rice, Chem. Rev. **94**, 3 (1994).
[60] V. Carravetta, Y. Luo, and H. Ågren, Chem. Phys. **174**, 141 (1993).
[61] R. van Leeuwen and E. J. Baerends, Phys. Rev. A **49**, 2421 (1994).
[62] R. van Leeuwen and E. J. Baerends, Phys. Rev. A **51**, 170 (1995).
[63] P. Jemmer and P. J. Knowles, Phys. Rev. A **51**, 3571 (1995).
[64] A. Lembarki, F. Rogemond, and H. Chermette (unpublished).
[65] G. Huber and G. Herzberg, *Spectra of Diatomic Molecules* (Van Nostrand, Princeton, 1979).
[66] G. D. Zeiss and W. J. Meath, Mol. Phys. **33**, 1155 (1977).
[67] M. A. Spackman, J. Chem. Phys. **94** 1288 (1991).